Design and performance of a compact, miniature static Fourier transform imaging spectropolarimeter

LI Jie a, ZHU Jing-ping a, WU Hai-ying b, HOU Xun a

^a Key Laboratory for Physical Electronics and Devices of the Ministry of Education & Shaanxi Key Lab of Information Photonic Technique, Xi'an Jiaotong University, Xi'an 710049, P.R. China simonli139@gmail.com

^b Huayin Ordnance Test Center, Huayin 714200, P.R. China

ABSTRACT

We propose a compact, miniature static Fourier transform imaging spectropolarimeter (SFTISP). The spectropolarimeter is formed by cascading two high order crystal retarders and a Wollaston birefringent interferometer. Compared with previous instruments, the most significant advantage of the described model is that without any internal moving parts, electrically controllable or micro-components, the entire wavelength-dependent state of polarization (SOP) is acquired simultaneously along a one-dimensional spatial image by a single snapshot. Also, we show that in this configuration we can benefit from the advantages of the element: compact, robust and high throughput of the Wollaston birefringent interferometer. The theory of the birefringent SFTISP is provided, followed by details of its specific embodiment. A simulation and an experimental demonstration of the sensor are also presented. The core optics of the breadboard sensor is as small as $8 \times \Phi$ 3.5 cm³ in size. The operation spectral range is from 450 nm to 850 nm. The experiment results were shown to yield accuracy better than 3% over most of the operation spectral band.

Keywords: Spectropolarimetry, Imaging spectropolarimeter, State of polarization, Fourier transform, Birefringent interferometer, Wollaston prism, Crystal retarders, Polarization detect, Interference, Interferogram.

1. INTRODUCTION

In recent ten years, spectropolarimetry has become a well-recognized technique in many fields, including biomedical optics, astronomy, remote sensing for object detection and identification ^[1, 2]. The conventional polarimeters generally suffer from vibration, electrical noise, heat generation, and alignment difficulty introduced by their rotating polarization elements, electrically controllable components, and microretarder or micropolarizer arrays. Consequently, considerable care is required for stable operation. Additionally, the incorporation of these mechanical components inevitably increases the complexity and decreases the reliability of the measurement system.

The channeled polarimetry, first proposed by K. Oka ^[3], is an attractive approach for polarization acquisition. Based on this concept, a variety of polarimeters have been developed for capturing polarization states of light ^[4-7]. K. Oka et al. developed a wedge imaging polarimeter employing monochromatic illumination ^[5]. M. W. Kudenov et al. provided a non-imaging system based on a mechanically scanned interferometer ^[7].

Developing the ideas above even further, we present a novel static imaging spectropolarimeter that combines channeled polarimetry with a birefringent interferometer ^[8]. Without any internal moving parts, electrically controllable or micro-components, the entire wavelength-dependent state of polarization (SOP), spectral and spatial information of a scene can be acquired simultaneously. Furthermore, the presented sensor is compact, robust and provides high radiometric throughput. Lastly, the interferometer has another unique benefit for working with the channeled polarimetry; namely, the Stokes vector is modulated directly into the interferogram, thus providing a more direct means of acquiring the wavelength-dependent SOP data.

2. PRINCIPLE OF OPERATION

The optical schematic of the SFTISP is illustrated in Fig. 1. Light from a scene is collected and collimated by the fore-optics, and then passes through a pair of birefringent retarders R₁ and R₂, and a polarizer P. The linearly polarized light emerging from P impinges on the Wollaston prism WP and is then equally split into two orthogonally polarized components with a small divergent angle. Successively, the two component rays traverse the analyzer A to be resolved into a common polarization state. Finally, reimaging lenses set on the exit port recombine the two rays onto the FPA at the focal plane. The FPA then records interferogram patterns along one dimension and 1D spatial imaging of the scene along the other dimension. 2D spatial imaging can be achieved by the "push-broom" mode scanning across a scene.

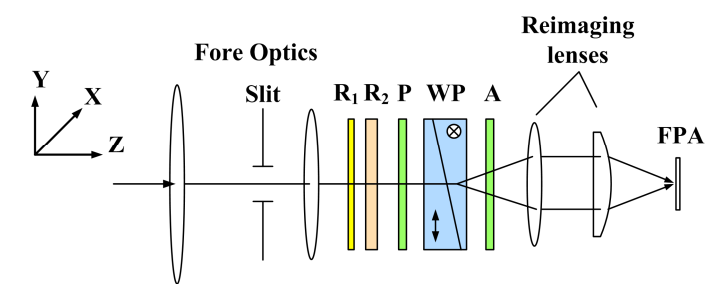


Fig.1. Schematic of the SFTISP. The optic axis of the Wollaston prism is indicated by arrow and circle.

The obtained interferogram of the SFTISP can be calculated by using the Mueller matrix theory. We assume that the light from the object have a broadband spectrum, and gradually changes with wave number σ from σ_1 =11764.71 cm⁻¹ to σ_2 =22222.22 cm⁻¹ (450-850nm). So the interferogram I(z) can be described as:

$$I(z) = \int_{\sigma_2}^{\sigma_1} \mathbf{MS}_i(\sigma) d\sigma , \qquad (1)$$

with

$$\mathbf{M} = \mathbf{M}_{A} \mathbf{M}_{WP} \mathbf{M}_{P} \mathbf{M}_{R}, \mathbf{M}_{R}, \qquad (2)$$

$$\mathbf{S}_{i}(\sigma) = (S_{0}(\sigma) \quad S_{1}(\sigma) \quad S_{2}(\sigma) \quad S_{3}(\sigma))^{\mathrm{T}}, \tag{3}$$

where z denotes the path difference introduced by the interferometer, **M** characterizes the collective polarimetric response of the sensor's polarization elements (R_1 , R_2 , P, WP and A); $S_i(\sigma)$ is the Stokes vector of the input light (where the superscript T represents the transpose operation). Thus, the obtained intensity pattern on the FPA can be given by:

$$I(z) = \int_{\sigma_2}^{\sigma_1} \frac{1 + \cos(\phi_z)}{4} \begin{cases} S_0 + \frac{1}{2} S_2 [\exp(i\phi_2) + \exp(-i\phi_2)] \\ + \frac{1}{4} [S_{13} \exp(i(\phi_1 - \phi_2)) + S_{13}^* \exp(-i(\phi_1 - \phi_2))] \\ - \frac{1}{4} [S_{13} \exp(i(\phi_1 + \phi_2)) + S_{13}^* \exp(-i(\phi_1 + \phi_2))] \end{cases} d\sigma ,$$

$$(4)$$

where $S_{13} = S_1 + iS_3$, and the superscript * denotes the complex conjugate; ϕ_z , ϕ_1 , and ϕ_2 are the phase retardations introduced by WP, R_1 and R_2 respectively. From Eq. 4, we can see that different phase factors are modulated onto the Stokes vectors of the input light. Performing the integration over σ , Eq. 4 can be rewritten as:

$$I(z) = \frac{1}{4}C_0(z) + \frac{1}{8}\left[C_2(z - L_2) + C_2^*(-z - L_2)\right] + \frac{1}{16}\left[C_1(z - (L_1 - L_2)) + C_1^*(-z - (L_1 - L_2))\right] - \frac{1}{16}\left[C_3(z - (L_1 + L_2)) + C_3^*(-z - (L_1 + L_2))\right]. \quad (5)$$

It can be known that the interferogram I(z) are separated into seven channels, centered at z = 0, $\pm (L_1 - L_2)$, $\pm L_2$, and $\pm (L_1 + L_2)$, where L_1 and L_2 denote the OPD originated by R_1 and R_2 .

By properly filtering the channels and performing the Fourier analysis, the input Stokes parameters can be demodulated as follows:

$$\mathsf{F}^{-1}(C_0) = \frac{1}{4} S_0(\sigma) \,, \tag{6}$$

$$\mathsf{F}^{-1}(C_1) = \frac{1}{16} (S_1(\sigma) + jS_3(\sigma)) \exp(j(\phi_1 - \phi_2)), \tag{7}$$

$$\mathsf{F}^{-1}(C_2) = \frac{1}{8} S_2(\sigma) \exp(j\phi_2) \ . \tag{8}$$

3. NUMERICAL SIMULATIONS

This section presents the numerical simulations of the above principle analysis. The Stokes parameters of the input light being measured are assumed to change with wave number σ from σ_1 =11764.71 cm⁻¹ to σ_2 =22222.22 cm⁻¹ (450-850nm), as shown in Fig. 2.

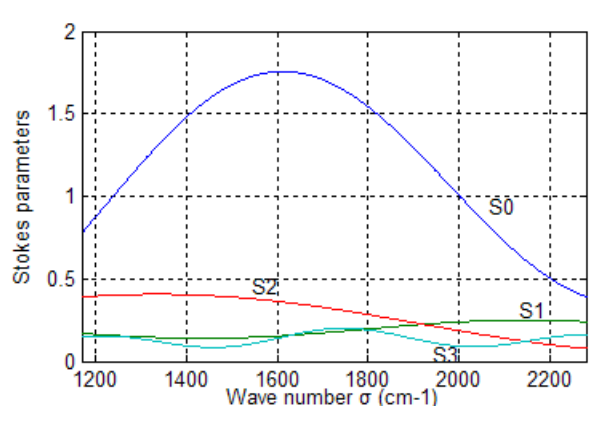


Fig.2. Stokes parameters of the input light produced by simulation.

The measured input light passes through the SFTISP and forms a channeled interferogram which is captured by FPA. This channeled interferogram is simulated by numerical calculating of Eq. 4 and illustrated in Fig. 3.

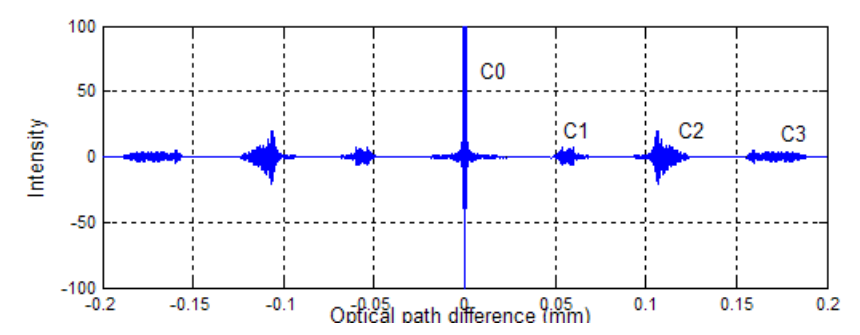


Fig.3. Intensity distribution of the simulated interferogram.

In the demodulation of the Stokes parameters, channels C_0 , C_1 , and C_2 in the interferogram are filtered, and then calculated by Eqs. 6-8 and results are presented in Fig. 4.

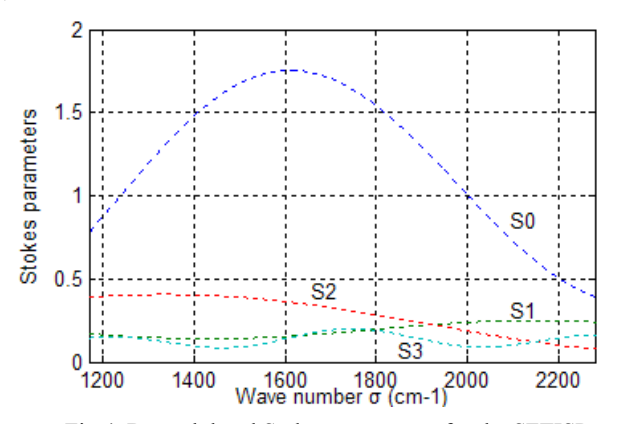


Fig.4. Demodulated Stokes parameters for the SFTISP.

4. EXPERIMENTAL DEMONSTRATION

We carried out an experiment to demonstrate the validity of our method. The experimental setup is illustrated in Fig. 5. A tungsten halogen lamp, a template (T) and a polarizer (P) are used to generate the polychromatic light being measured. In the developed scheme, the Wollaston prism is made of calcite. The core optics of the developed imaging spectropolarimeter, shown in Fig. 6, is less than $8\times\Phi$ 3.5 cm³ in size (without imaging optics). We use a low-cost 8-bit CMOS camera to take the interferogram and 1D imaging of the target T.

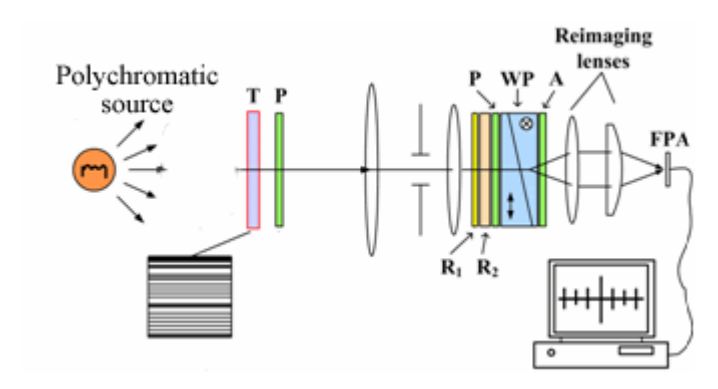


Fig.5. Experiment setup of the developed imaging spectropolarimeter.

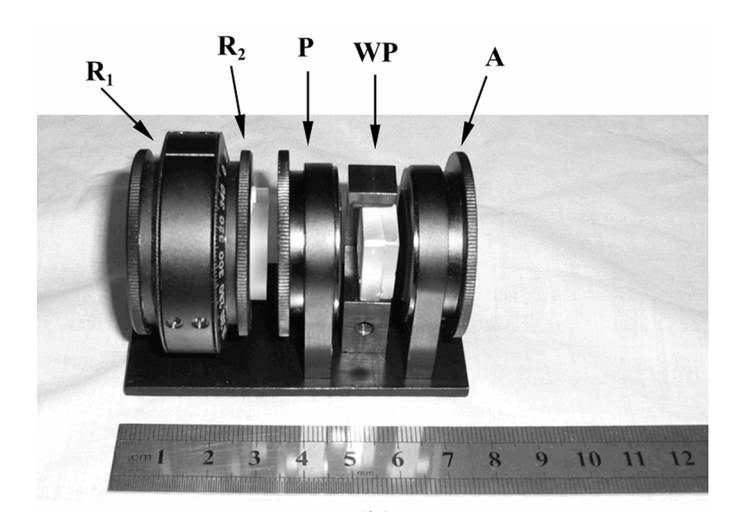


Fig.6. Photograph of the core optics.

The obtained interferogram is shown in Fig. 7. It can be seen that three channels C_0 , C_1 *, and C_2 * are successfully separated from one another. All the wavelength dependent SOP (i.e. $S_0(\sigma)$, $S_1(\sigma)$, $S_2(\sigma)$, $S_3(\sigma)$) can be demodulated from these channels. Note that the Stokes parameter $S_0(\sigma)$ is the intensity spectrum of the incident light. Fig. 8(a) depicts the demodulated spectrum $S_0(\sigma)$, while Fig. 8(b) provides the normalized SOP quantities. Compared with the theoretical values, the experimental results exhibit favorable accordance and the feasibility of the present idea is validated. Here the polarization accuracy can reach better than 3% over most of the 450-850 nm bands. And the accuracy could be effectively improved with further development and calibration refinement.

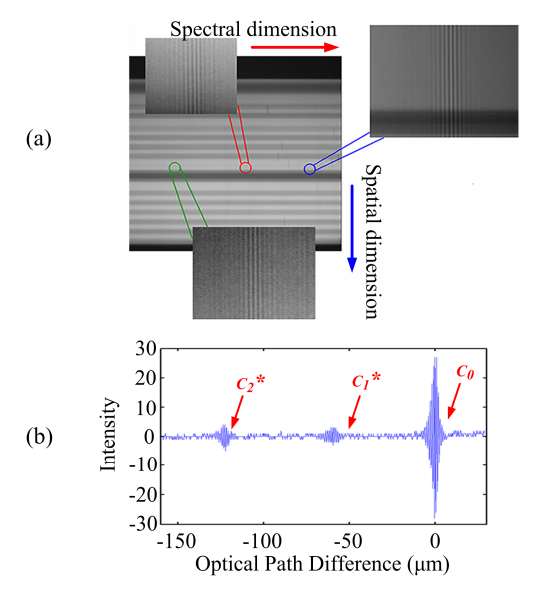


Fig.7. Interferogram captured by the described spectropolarimeter with the input Stokes parameters.

(a) Original patterns (b) intensity distribution of a single point.

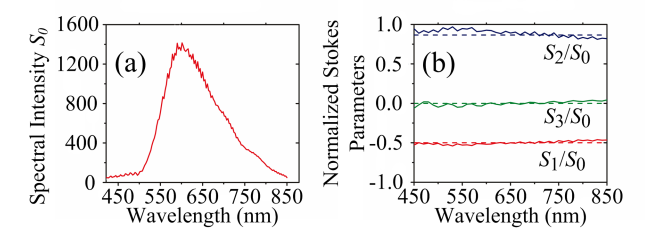


Fig. 8. (a) Demodulated spectrum $S_0(\sigma)$, (b) normalized Stokes parameters.

Solid and dashed lines show the experimental and theoretical values, respectively.

5. CONCLUSION AND FUTURE WORKS

The proposed imaging spectropolarimeter implies many advantages due to its compactness, simple configuration, static nature, robust and low cost. With this setup, all the wavelength-dependent SOP, spectral and 1D spatial imaging of objects can be obtained with a single snapshot. Besides, 2D image information of the object can be acquired by the "push-broom" mode. Furthermore, the presented sensor derives three advantages from the birefringent interferometer: 1) High optical throughput. The sensor's spectral resolution is independent on the width of the input slit aperture; 2) Broad wavelength range. The spectral bandwidth is limited only by the spectral response of the detector array and the crystal's birefringence (the transmission wavelength of calcite is from 215 nm~2.3 µm which is covered the working band of the CCD detector); 3) High wavelength accuracy. The interferometer can generally yield more accurate spectra than the dispersive spectrometer.

It should be indicated that, because of the polarizer and analyzer, the optical efficiency of the demonstrated sensor is about 25%. As an alternative, the interference element could be replaced by an analyzer-less interferometer, for example, the Sagnac or triangle-path interferometer. However, due to the reflection on the beam splitter and mirrors in this case, the optical efficiency is the same as the demonstrated sensor. To overcome this shortcoming, we are planning to propose

a spectropolarimeter based on an interferometer with no analyzer or mirrors. Once completed, a comparison analysis of the signal-to-noise ratio and SOP demodulation algorithms of these higher-throughput instruments will be presented.

6. REFERENCES

- [1] W. Groner, J. W. Winkelman, A. G. Harris *et al.*, "Orthogonal polarization spectral imaging: A new method for study of the microcirculation," Nature Medicine, 5(10), 1209-1213 (1999).
- [2] L. F. Wang, D. Baade, and F. Patat, "Spectropolarimetric diagnostics of thermonuclear supernova explosions," Science, 315(5809), 212-214 (2007).
- [3] K. Oka, and T. Kato, "Spectroscopic polarimetry with a channeled spectrum," Optics Letters, 24(21), 1475-1477 (1999).
- [4] A. M. Locke, D. S. Sabatke, E. L. Dereniak *et al.*, "Snapshot imaging spectropolarimeter," Proc. SPIE 4481, 64-72 (2002).
- [5] K. Oka, and T. Kaneko, "Compact complete imaging polarimeter using birefringent wedge prisms," Optics Express, 11(13), 1510-1519 (2003).
- [6] K. Oka, S. Endo, A. Taniguchi *et al.*, "Channeled spectroscopic polarization state generator (CSPSG) and its application to spectroscopic measurement of Mueller matrix," Proc. SPIE 6682, 68203-68203 (2007).
- [7] M. W. Kudenov, N. A. Hagen, E. L. Dereniak *et al.*, "Fourier transform channeled spectropolarimetry in the MWIR," Optics Express, 15, 12792-12805 (2007).
- [8] J. Li, J. Zhu, and H. Wu, "Compact static Fourier transform imaging spectropolarimeter based on channeled polarimetry," Optics Letters, 35(22), 3784-3786 (2010).

Proc. of SPIE Vol. 8191 81911C-7